Decomposition Pathways of Peroxynitrous Acid: Gas-Phase and Solution Energetics

David A. Dixon,* David Feller, and Chang-Guo Zhan

William R. Wiley Environmental Molecular Sciences Laboratory, Pacific Northwest National Laboratory, P.O. Box 999, Richland, Washington 99352

Joseph S. Francisco

Department of Chemistry, H. C. Brown Laboratory, Purdue University, West Lafayette, Indiana 47907-1393

Received: October 10, 2001; In Final Form: January 17, 2002

It was recently suggested that HOONO, which forms after protonation of the $ONOO^-$ anion under biological conditions, decomposes into HNO and $(^1\Delta_g)O_2$. Subsequent workers argued that the mechanism for HOONO decomposition proceeds via homolytic bond fission, producing the radical pair OH and NO_2, and another recent study argued that a cyclic form of the peroxynitrous acid results in the products $H^+ + O_2(^1\Delta_g) + NO^-$. Calculations on the reaction pathway for the process showed that it required a high activation energy, and is thus implausible. High level ab initio molecular orbital theory including extrapolation to the complete basis set limit has been used to calculate the heats of formation of reactants and products for the homolytic bond fission pathways for decomposition of HOONO and the molecular pathway that yields HNO and $^1O_2$ as well as the transition state for the latter process. These data are used to evaluate the probability of whether the decomposition of peroxynitrous acid can produce HNO and $^1O_2$. Isomerization of HOONO to $HONO_2$ is also discussed.

Introduction

Peroxynitrous acid (HOONO) is a key intermediate that is important in biological processes, the deprotonation of which yields peroxynitrite ($OONO^-$), a potent oxidant of biomolecules. Peroxynitrite can also be formed from the reaction of superoxide and nitrogen monoxide[1,2] and, upon protonation, forms HOONO. The mechanism by which biomolecules are oxidized by these species is the focus of much current research.[3−12] A number of short papers summarizing some of this work were recently published in a forum in *Chemical Research in Toxicology*.[13−19] An important question in recent research is how the peroxynitrous acid (HOONO) decomposes once it is formed. Mahoney[20] originally suggested that peroxynitrous acid decomposes into a radical pair, OH and NO_2. For nearly 20 years, thermodynamic estimates that were not reliable gave rise to much confusion along with misinterpretation of various experiments.[11,13−19,21−23] Recent experiments support the radical pair mechanism whereas others do not.[13−19,24−28] Khan et al.[26] reported that upon protonation of peroxynitrite, the peroxynitrous acid decomposes into $(^1\Delta_g)O_2$ and HNO and proposed that the reaction proceeds via a four-membered ring structure. The resulting products exhibit spin-conservation on the singlet potential energy surface. It was suggested that HNO deprotonates to form the oxonitrate[1] ion (NO^-) at pH 7.0 on the basis of the reported pK_a of HNO as being 4.7 although recent theoretical work[27] has suggested a higher pK_a of 7.2. Evidence for this mechanism is the formation of nitrosylhemoglobin (HbNO) under biological conditions. Merenyi et al.[28] argued on thermodynamic grounds that the decomposition of HOONO cannot proceed by formation of HNO and $(^1\Delta_g)O_2$, but instead proceeds via the formation of the radical pair OH and NO_2. These authors then suggest that at least 70% of the radical pair recombines in the solvent cage to nitric acid ($HONO_2$). The nitric acid can then deprotonate to give NO_3^-. Martinez et al.[29] showed in recent experiments that evidence presented by Khan et al.[26] is based on misinterpreted UV−visible spectra. Martinez et al.,[29] following a suggestion of Khan et al.,[26] performed calculations that the proposed four-center transition state is actually an intermediate for peroxynitrous acid to form HNO and $(^1\Delta_g)O_2$ and occurs at high energy. However, the four-center intermediate proposed to Khan et al.[26] is not the simplest chemical one in that the hydrogen is on the nitrogen and there is oxygen transfer in the transition state. It is not clear how the hydrogen transfers from the oxygen of HOONO to the nitrogen. The transition state structure for the formation of HNO and $(^1\Delta_g)O_2$ from HOONO proposed by Khan et al.[26] and calculated to be an intermediate by Martinez et al.[29] is probably not representative of the lowest energy process and, hence, cannot be used to argue the case against Khan et al.[26] Other recent work by Ingold's group[24,25] has shown that not very much free OH is formed on the decomposition of HOONO by O−O bond scission, although they do note that a distinct pathway leading to formation of OH is present. Rather, the radical pair remains trapped in a solvent cage and rearranges to form $HONO_2$ 90% of the time.

To examine whether decomposition of peroxynitrous acid proceeds via a radical pair mechanism or via a molecular rearrangement leading to elimination of HNO and $(^1\Delta_g)O_2$, high level ab initio electronic structure calculations have been performed to predict the barrier heights and accurate thermochemical properties of species involved in the decomposition reaction of peroxynitrous acid.

Results and Discussion

In an effort to predict uniformly accurate thermochemical properties across a range of small-to-intermediate size chemical

* Author to whom correspondence should be addressed.

10.1021/jp013783z CCC: $22.00
Published on Web 03/08/2002

TABLE 1: Energy Decomposition for Calculating Heats of Formation (in kcal mol^{-1})

molecule	$\sum D_e$(elec)[a]	ΔE_{CV}[b]	ΔE_{SR}[c]	ΔE_{SO}[d]	$\sum D_e$	ZPE[e]	$\sum D_0$
OH	107.20	0.14	−0.13	−0.11	107.10	5.28	101.82
HO_2	174.46	0.22	−0.37	−0.43	173.88	8.61	165.27
HNO	205.26	0.39	−0.18	−0.21	205.26	8.77	196.49
NO	151.92	0.36	−0.08	−0.05	152.15	2.71	149.44
NO_2	226.16	0.63	−0.59	−0.43	225.77	5.40	220.37
O_2	119.89	0.21	−0.25	−0.43	119.42	2.25	117.17
HOONO	356.94	0.87	−0.83	−0.64	356.34	14.35	341.99
$HONO_2$	387.77	1.29	−1.02	−0.64	387.40	16.43	370.97
HOONO(TS1)	304.20	1.03	−0.85	−0.64	303.74	12.75	290.99
HOONO(TS2)	333.52	0.54	−0.78	−0.64	332.64	12.05	320.59

[a] Mixed Gaussian extrapolation of CCSD(T)/aug-cc-pVXZ energies, X = D, T, Q to complete basis set limit (CBS) valence electronic energies. [b] Core-valence electronic energy corrections. [c] Scalar-relativistic electronic energy corrections. [d] Spin−orbit energy corrections. [e] Zero point energy corrections. See text for details.

systems, we have developed a composite theoretical approach without recourse to empirical parameters.[30] This approach starts with existing, reliable thermodynamic values obtained from either experiment or theory. Normally we adopt experimental atomic heats of formation, which are difficult to obtain theoretically, as well as molecular and atomic spin−orbit splittings (if any) and use experimental information about molecular vibrations to calculate zero point energies where possible. High-level ab initio electronic structure methods are then used to complete the calculation of the molecular atomization energy.

The energy of the valence electrons is calculated by using coupled cluster methods, including single, double, and connected triple excitations (CCSD(T)), with the latter being handled perturbatively.[31] The CCSD(T) energies are extrapolated to the complete basis set (CBS) limit, a step facilitated by the uniform convergence properties of the correlation consistent basis sets (cc-pVXZ) from Dunning and co-workers.[32] For this study, we used the diffuse function augmented (aug-cc-pVXZ) basis sets for X = D, T, and Q. For the sake of brevity, the basis set names will be shortened to aVxZ throughout this text. Only the spherical components (5-3, 7-f, and 9-g) of the Cartesian basis functions were used. All of the current work was performed with the programs MOLPRO, NWChem, and Gaussian98.[33]

Three coupled cluster methods have been proposed for treating open-shell systems. The first is a completely unrestricted method, built atop unrestricted Hartree−Fock (UHF) orbitals and designated UCCSD(T). The other two methods start with restricted open-shell Hartree−Fock (ROHF) orbitals. One is a completely restricted method, which we label as RCCSD(T).[34] The other relaxes the spin constraint in the coupled cluster calculation and is designated R/UCCSD(T).[35] At present, little is known about which open-shell coupled cluster method produces the best agreement with the exact full configuration interaction (FCI) results. We have used the RCCSD(T) and R/UCCSD(T) methods in this study. For the closed-shell molecules, we have used the R/UCCSD(T) atomic energies.

To extrapolate to the frozen core CBS limit, we used a 3-parameter, mixed exponential/Gaussian function of the following form:

$$E(x) = A_{CBS} + B \exp[-(x-1)] + C \exp[-(x-1)^2] \qquad (1)$$

where $x = 2$ (DZ), 3 (TZ), etc.[36] This form is appropriate when basis sets up through aVQZ are used.

The geometries were optimized at the CCSD(T) level except for HOONO and $HONO_2$, where the geometries were obtained at the MP2/cc-pVTZ level[37] of theory. We also optimized the geometry at the CCSD(T)/aug-cc-pVDZ level for $HONO_2$ and HOONO and used these geometry parameters for total energy extrapolations. Use of these geometries which did not differ in a significant way from the MP2/cc-pVTZ geometries led to extrapolated total valence electronic binding energies that were 0.56 and 0.70 kcal/mol smaller than the ones based on the MP2 optimized geometries for $HONO_2$ and HOONO, respectively. Table 1 shows the various energy components used in calculating the total dissociation energies for OH, HO_2, HNO, NO, NO_2, O_2, and HOONO, as well as the convergence of the valence shell component of the corresponding dissociation energies. The molecular zero point energy was obtained, as follows. For the diatomics, the zero point energies were evaluated as $0.5\omega_e - 0.25\omega_e x_e$, where the ω_e and $\omega_e x_e$ values were taken from Huber and Herzberg.[38] For HO_2, the zero point energy was taken as one-half of the average of the experimental anharmonic values[39] and the harmonic values calculated at the CCSD(T)/aVDZ level. For NO_2, we took the zero point energy to be one-half the sum of the experimental fundamental (anharmonic) frequencies.[40] For $HONO_2$, we used the average of the experimental anharmonic frequencies[40] with the MP2/cc-pVTZ harmonic frequencies. For HOONO, we calculated the frequencies at the QCISD/cc-pVDZ (quadratic configuration interaction with singles and doubles)[41] and MP2/cc-pVTZ levels. Experimental values[42] are available for the six highest out of the nine possible modes of HOONO. For the OH stretch, we took the average of the two calculated values and averaged it with the experimental value. We then used the experimental values for the next five modes, and for the three lowest modes we used the average of the calculated values and calculated the zero point energy as one-half the sum of all of these values.

Additional corrections to the CCSD(T)(FC) atomization energies are needed when trying to achieve accuracies on the order of a kcal mol^{-1}. Core/valence corrections (ΔE_{CV}) to the dissociation energy were obtained from fully correlated CCSD(T) or RCCSD(T) calculations with the cc-pCVQZ basis set[32] performed at the optimal CCSD(T)/aug-cc-pVTZ geometry except for HOONO and $HONO_2$. For HOONO and $HONO_2$, ΔE_{CV} was calculated at the CCSD(T)/cc-pCVTZ level. The effects of relativity must also be considered. Most electronic structure computer codes do not correctly describe the lowest energy spin multiplet of an atomic state. Instead, the energy is a weighted average of the available multiplets. For N in the ^{4}S state, no such correction is needed, but a correction is needed for the ^{3}P state of O. To correct for this effect, we apply an atomic spin−orbit correction of −0.22 kcal mol^{-1} for O based on the excitation energies of Moore.[43] For OH and NO, the spin−orbit corrections are from Huber and Herzberg.[38] Molecular scalar relativistic corrections (ΔE_{SR}), which account for changes in the relativistic contributions to the total energies of

TABLE 2: Calculated and Experimental Heats of Formation (in kcal mol^{-1})

molecule	ΔH_f(calc, 0 K)	ΔH_f(expt, 0 K)[a]
OH	8.79	8.82,[b] 9.18
HO_2	4.32	4.20 +1.0/−0.5,[d] 3.5 ± 0.5,[c] 1.2 ± 2
HNO	26.65	26.3 ± 1,[c] 24.5
NO	22.07	21.46 ± 0.04
NO_2	10.12	8.59 ± 0.2
O_2	0.79	0.0
$HONO_2$	−29.87	−29.75 ± 0.1
HOONO	−0.89	

[a] Experimental values are from ref 45 unless otherwise noted. [b] Ruscic, B.; Feller, D.; Dixon, D. A.; Peterson, K. A.; Harding, L. B.; Asher, R. L.; Wagner, A. F. *J. Phys. Chem. A* **2001**, *105*, 1. [c] Value at 298 K from ref 48 corrected to 0 K by use of ref 45. [d] Ref 46.

the molecule and the constituent atoms, were included at the CI-SD level of theory using the cc-pVTZ basis set in the frozen core approximation. ΔE_{SR} is taken as the sum of the mass−velocity and one-electron Darwin (MVD) terms in the Breit−Pauli Hamiltonian.[44]

By combining our computed D_0 values with the known[45] heats of formation at 0 K for the elements (ΔH_f^0(N) = 112.53 kcal mol^{-1}, ΔH_f^0(O) = 58.98 kcal mol^{-1}, and ΔH_f^0(H) = 51.63 kcal mol^{-1}), we can derive ΔH_f^0 values for the molecules under study as shown in Table 2. For all of the molecules whose heats of formation are known, except for NO_2, the difference between the calculated and experimental values is less than 1 kcal mol^{-1}. For NO_2, the difference is 1.5 kcal mol^{-1}, somewhat larger than what we would have expected, but still in reasonable agreement with the experimental value. The difference from experiment for NO_2 is likely due to the complicated bonding in this open shell doublet and is about double the error in the heats of formation of NO or O_2. We note that our calculated heat of formation for HO_2 does confirm the more recent value given by Shum and Benson[46] and shows that the usually accepted JANAF value[45] does need to be revised. In addition, our calculated value of 4.36 kcal/mol for $\Delta H_f^0(HO_2)$ is in good agreement with the value of 3.50 kcal/mol based on CCSD(T)/aug-cc-pVQZ and CCSD(T)/cc-pV5Z calculations of the H−O bond energy in HO_2 with an empirical correction.[47] We would obtain a value of 3.57 kcal/mol for $\Delta H_f^0(HO_2)$ at 0 K based on our calculated H−O bond energy in excellent agreement with the Bauschlicher and Partridge value.[47] In addition, our calculated value for $\Delta H_f^0(HO_2)$ is in good agreement with the value of 3.5 ± 0.5 kcal/mol from the NASA compilation[48] corrected to 0 K.[45] The calculated value for HOONO is in reasonable agreement with the G2[49] calculated value[50] of −3.6 kcal/mol at 0 K and the estimated heat of formation of 1.1 ± 1 kcal/mol from Richeson et al.[24] where we have corrected their 298 K value using the correction given by McGrath and Rowland.[50] The G2 value[51] for HNO_3 corrected to 0 K is −32.4 kcal/mol, somewhat too negative as compared to our value.

We performed a conformational search on HOONO. The lowest energy structure is the cis structure in a ring form where a hydrogen bond is present between the H and the terminal O bonded to N. The next highest energy structure is the open structure resembling HOOH with the NO out of the HOO plane. This structure is 3.69 kcal mol^{-1} higher in energy at the CCSD(T)/CBS level, showing that a reasonably strong internal hydrogen bond is present in the most stable structure. The cis structure obtained by rotating the NO group by 180° is not a minimum energy structure (it is characterized by one imaginary frequency at the MP2/cc-pVTZ level) and is 6.45 kcal mol^{-1} above the energy of the optimal cis structure, again showing the presence of a strong hydrogen bond in the lowest energy structure. This latter structure is the one which can transfer the hydrogen to the nitrogen. The predicted structures are in reasonable agreement with calculations at the density functional theory, MP2, and CCSD levels.[50,51]

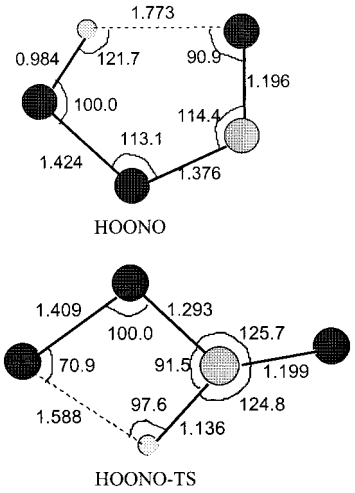

Figure 1. Geometries of the lowest energy form of HOONO and the transition state leading to HNO + $O_2(^1\Delta_g)$ (TS1) optimized at the MP2/cc-pVTZ level. Key geometric parameters are given, distances in Å and angles in degrees.

We calculated the transition state for the unimolecular decomposition of HOONO into HNO and $(^1\Delta_g)O_2$. The transition state (TS1) is characterized by the transfer of the H to the N in a four-center process. (See Figure 1) The N−H bond is already strongly formed in the TS, and the original OH bond is essentially broken. The O_2 has not left the N, and the O_2 π bond has not yet formed. The transition state is planar and is characterized by an imaginary frequency of 1084i cm^{-1} at the MP2/cc-pVTZ level. The TS is 52.60 kcal mol^{-1} above HOONO at the CCSD(T)/CBS level, including scalar relativistic and core-valence corrections. To obtain a zero point energy difference, we used a scale factor of 0.97 for the transition state calculated frequencies obtained as the average of the scale factors of the MP2 results for $HONO_2$ and HOONO. This energy is reduced to 51.0 kcal mol^{-1} at 0 K when the scaled zero point energy correction is included. We used the Intrinsic Reaction Coordinate (IRC) approach[52,53] to show that the transition state leading to HNO + O_2 ($^1\Delta$) products does indeed correlate with the $^1\Delta_g$ state as compared to the $^1\Sigma_g^+$ state based on single reference wave functions. This is consistent with the fact that the $^1\Sigma_g^+$ state lies 15.1 kcal/mol above the $^1\Delta_g$ state.[38]

The two lowest energy pathways for the decomposition of peroxynitrous acid are predicted to form the radical pairs: (1) OH + NO_2 and (2) HO_2 + NO. The 0 K heats of reaction are predicted to be 19.8 and 27.3 kcal mol^{-1}, respectively, as shown in Table 3. The next highest energy path is the spin-forbidden formation of HNO + $(^3\Sigma_g^-)O_2$ (where the O_2 is in its ground state), predicted to be 28.3 kcal mol^{-1}. The highest energy pathway is formation of HNO + $(^1\Delta_g)O_2$, 31 kcal mol^{-1} above the lowest energy OH + NO_2 channel where we have used the experimental energy difference between $(^3\Sigma_g^-)O_2$ and $(^1\Delta_g)O_2$. The calculations clearly show that on energetic grounds the unimolecular decomposition of HOONO to yield HNO and $(^1\Delta_g)O_2$ is the least favored pathway, consistent with the studies of Merenyi and co-workers[12,15,22,28,54] and others.[24,25,55] The transition state for formation of $(^1\Delta_g)O_2$ and HNO is essentially the same energy as the exothermicity of the process.

Our conclusions are based on very accurate gas-phase reaction energies, and one can argue that the studies in question have

TABLE 3: Reaction Energies (in kcal mol^{-1})

reaction	all calc ΔH(0 K)	expt[a] ΔH(0 K)	$\Delta\Delta H$ (298)	$-T\Delta S$ (298)	ΔG (298)	ΔG (298)[b] solv	ΔG (298) soln	ΔG(298)[c] soln(expt)
HOONO → HNO + ($^3\Sigma_g^-$)O_2	28.3	27.2	+1.4	−10.4	19.3	−0.7	19.0	
→ HNO + ($^1\Delta_g$)O_2	50.8	49.7					(41.5)[d]	
→ OH + NO_2	19.8	18.3	+1.4	−10.1	11.1	−2.2	8.9	13.6
→ HO_2 + NO	27.3	26.6	+1.4	−10.8	17.9	−3.1	14.8	17.8
→ $HONO_2$	−29.0	−28.9	−0.2	0.6	−28.6	−4.1	−32.7	−32.4
→ TS1	51.0							
→ TS2	21.4							

[a] Experimental values from Table 2 (first value) except for ΔH_f(HOONO) for which the calculated value was used. [b] Solvation effects at 298 K from MP2/cc-pVTZ reaction field calculations. See text. [c] See text for details relating to experimental values in solution. [d] Calculated assuming no solvation effect on the singlet−triplet splitting.

all been done in solution. We have examined the effect of solvation on the gas-phase energetics to see if this effect can shift the energetics in favor of the HNO + ($^1\Delta_g$)O_2 pathway. Solvent shifts of the energies were evaluated by using a recently developed GAMESS[56] implementation of the surface and volume polarization for electrostatic interactions (SVPE).[57] The SVPE model is known as the fully polarizable continuum model (FPCM)[58,59] because it fully accounts for both surface and volume polarization effects in the self-consistent reaction field (SCRF) calculation. Since the solute cavity surface is defined as a solute electron charge isodensity contour determined self-consistently during the SVPE iteration process, the SVPE results, converged to the exact solution of Poisson's equation with a given numerical tolerance, depend only on the contour value at a given dielectric constant and a certain quantum chemical calculation level.[57a] This single parameter value has been calibrated as 0.001 au[57b] and this contour was used for all of the SVPE calculations. Previous continuum solvation calculations with the SVPE method indicate that electron correlation effects on the solvent shifts calculated by the SVPE method are not important.[60] This issue was further examined in the present study by performing the SVPE calculations at both the HF/cc-pVTZ and MP2/cc-pVTZ levels. The dielectric constant of water used in this study is 78.5. The results of the solvation calculations for the free energy of the reaction, ΔG(298), are given in Table 3. We calculated the gas-phase entropies and the corrections for converting the enthalpy to 298 K at the gradient-corrected density functional theory level.[61] The largest effect is the $T\Delta S$ term to convert the enthalpy to a free energy in the gas phase and is on the order of 10 to 11 kcal mol^{-1}. The solvation free energy effects are much smaller, 1.0 to 3.0 kcal mol^{-1}. We can make the reasonable assumption that the corrections for ($^1\Delta_g$)O_2 are similar to those for ($^3\Sigma_g^-$)O_2 and there is no change in the ordering of the reaction energies. Thus, the conclusions derived from the accurate gas-phase values remain valid and, on the basis of thermodynamics, ($^1\Delta_g$)O_2 and HNO cannot be produced in the decomposition of HOONO at 298 K without an additional source of energy as the reaction is predicted to be more than 40 kcal mol^{-1} endothermic in aqueous solution. We note that the largest solvent shift (−5.8 kcal mol^{-1}) is predicted for the transition state to form ($^1\Delta_g$)O_2 and HNO as it has the largest dipole moment and the second largest is for the transformation of HOONO into $HONO_2$ favoring formation of the $HONO_2$ by an additional −4.1 kcal/mol.

We can compare our calculated free energies at 298 K with proposed experimental values. The free energy of formation of HOONO in aqueous solution at 298 K has been derived to be 7.7 kcal/mol.[12,15] We can combine this with provisional free energies of formation[62] in aqueous solution at 298 K for the radicals NO (24.4 kcal/mol), OH (6.2 kcal/mol), HO_2 (1.1 kcal/mol), and NO_2 (15.1 kcal/mol) to obtain experimental values for the bond dissociation energies in solution. The experimental bond energies are higher than our calculated values by 4.7 kcal/mol for the O−O bond and 3.0 kcal/mol for the N−O bond. The reasons for the discrepancies are either difficulties in calculating the solvation component or errors in the provisional experimental values. We note that a Car−Parrinello simulation using the BLYP functional did not find the cis structure with the internal hydrogen bond to be a stable structure in aqueous solution.[63] Rather the cis and trans structures of HOONO where the hydrogen is exposed to the solvent and can form a hydrogen bond to the water are the stable structures. It is possible that this in part could account for discrepancies of a few kcal/mol. However, we do find excellent agreement between theory and experiment for the isomerization reaction of HOONO to $HONO_2$, which suggests that the errors in the solvation of the two species are similar. Given the quite different structures and hydrogen bonding capabilities of the two species, it is surprising that the errors due to the solvation energy for the two structures are so similar.

Previous thermodynamic and kinetic studies have proposed that peroxynitrous acid, HOONO, isomerizes unimolecularly to nitric acid, $HONO_2$.[11,24,25,64] $HONO_2$ is calculated to be 29 kcal mol^{-1} more stable than HOONO so the isomerization is very exothermic. Two transition states for the isomerization of HOONO have been reported in the literature. The first transition state, reported by Cameron et al.,[65] was obtained at the Hartree−Fock(HF)/6-31G* level and goes to the correct reactants and products when an IRC analysis[52,53] is used to verify the transition state. Starting from this transition state and using higher levels of theory, we were unable to converge to a first-order saddle point. The other transition state is that obtained by Sumathi and Peyerimhoff[66] by using density functional theory (DFT, B3LYP/6-311+G**) who calculated an energy barrier to isomerization of 39.0 kcal mol^{-1}. The Cameron et al.[64] transition state and the Sumathi and Peyerimhoff[66] transition states for the HOONO isomerization to $HONO_2$ are very different. Houk and co-workers[67] have reported that at the B3LYP/6-31G* level they were unable to find a concerted transition state for this process, but rather that there are hydrogen-bonded complexes of OH with NO_2. We reoptimized the transition state for transfer of the OH group from O in HOONO to N to form $HONO_2$ (TS2) at the MP2/cc-pVDZ level and note that the transition state was very difficult to obtain. The transition state resembles an OH weakly coupled to NO_2 with an N−O(H) bond length of 2.78 Å and O−O bond lengths of 3.36 and 3.42 Å. (see Figure 2) The calculated energy of the isomerization transition state is 21.4 kcal mol^{-1} above that of HOONO at the CBS limit with all corrections. The energy to form the OH + NO_2 channel is less than 20 kcal mol^{-1}, 19.8 kcal mol^{-1} if all calculated values are used and 18.3 kcal mol^{-1} if mostly experimental values are used. The energetics combined with the geometry information are consistent with isomerization of HOONO to $HONO_2$ proceeding via the formation of the radical-pair OH and NO_2.

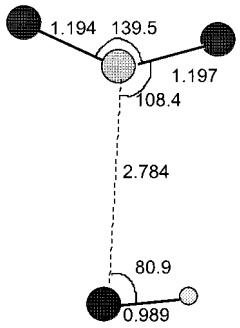

Figure 2. Geometry of the transition state for transfer of the OH group from O in HOONO to N to form $HONO_2$ (TS2) optimized at the MP2/cc-pVTZ level. Key geometric parameters are given, distances in Å and angles in degrees.

The two radicals are only weakly coupled at best so the mechanism can be considered a fully dissociative one. In solution, the isomerization would take place in a solvent cage which would facilitate the recombination, which is consistent with the conclusions of Merenyi et al.[28] and of Ingold and co-workers.[24,25]

Conclusion

There is no low energy channel in the dissociation of peroxynitrous acid that leads to the formation of HNO and $^1O_2$, either in the gas phase or solution. This conclusion argues against that of Khan et al.[26] The lowest energetic pathway is the formation of the radical pair ($OH + NO_2$) which can recombine in solution to form $HONO_2$ which then can deprotonate to form NO_3^-. Our findings are consistent with the findings of Merenyi et al.[28] Athough the emphasis of this work has been to evaluate the energetics of the decomposition of HOONO in solution, the gas-phase energetics presented in this work are relevant to on-going issues in the literature regarding the potential role of HOONO in NO_x partitioning in the atmosphere. Experiments aimed at measuring the binding energy of HOONO with respect to $OH + NO_2$ should find the present results important.[68]

Acknowledgment. The work at Pacific Northwest National Laboratory (PNNL) was supported in part by the U.S. Department of Energy, Offices of Basic Energy Sciences, Division of Chemical Sciences and Biological and Environmental Research (PNNL), under Contract No. DE-AC06-76RLO 1830 for PNNL and in part by a subcontract to Battelle Pacific Northwest Division from Oregon Health Sciences University under the auspices of a National Institute of Environmental Health Sciences Superfund Basic Research Center award. Part of this research was performed in the William R. Wiley Environmental Molecular Sciences Laboratory (EMSL) at the PNNL and some of the calculations were run in the Molecular Sciences Computing Facility. The EMSL is a national user facility funded by the Office of Biological and Environmental Research in the U.S. Department of Energy. PNNL is a multiprogram national laboratory operated by Battelle Memorial Institute for the U.S. Department of Energy.

References and Notes

(1) Huse, R. E.; Padmaja, S. *Free Radical Res. Commun*. **1993**, *18*, 195.

(2) Beckman, J. S.; Koppenol, W. H. *Am. J. Physiol. Cell Physiol*. **1996**, *271*, C1424.

(3) Ignarro, L. J.; Buga, G. M.; Wood, K. S.; Byrns, R. E.; Chaudhari, G. *Proc. Natl. Acad. Sci. U.S.A.* **1987**, *84*, 9265.

(4) Beckman, J. S.; Beckman, T. W.; Chen, J.; Marshall, P. A.; Freeman, B. A. *Proc. Natl. Acad. Sci. U.S.A.* **1990**, *87*, 1620.

(5) White, R. C.; Brock, T. A.; Chang, L.; Craps, J.; Brisco, P.; Ku, D.; Bradley, W. A.; Gianturco, S. H.; Gare, J.; Freeman, B.; Tarpey, M. M. *Proc. Natl. Acad. Sci. U.S.A.* **1994**, *91*, 1044.

(6) Lymar, S. V.; Aurst, J. K. *J. Am. Chem. Soc.* **1995**, *117*, 8867.

(7) Xia, Y.; Dawson, U. L.; Dawson, T. M.; Synder, S. H.; Zweier, J. L. *Proc. Natl. Acad. Sci. U.S.A.* **1996**, *93*, 6770.

(8) Xia, Y.; Zweier, J. L. *Proc. Natl. Acad. Sci. U.S.A.* **1997**, *94*, 6954.

(9) Fukuto, J. M.; Ignarro, L. G. *Acc. Chem. Res.* **1997**, *30*, 149.

(10) Vasquez-Vivar, J.; Kalyanaraman, B.; Martasek, P.; Hogs, N.; Masters, B. S. S.; Karoui, H.; Torodo, P.; Pritchard, K. A. *Proc. Natl. Acad. Sci. U.S.A.* **1998**, *95*, 9220.

(11) Koppenol, W. H.; Moreno, J. J.; Pryor, W. A.; Ischiropoulos, H.; Beckman, J. S. *Chem. Res. Toxicol.* **1992**, *5*, 834.

(12) Merenyi, G.; Lind, J. *Chem. Res. Toxicol*. **1998**, *11*, 243.

(13) Marnett, L. J. *Chem. Rev. Toxicol.* **1998**, *11*, 709.

(14) Bartberger, M. D.; Olson, L. P.; Houk, K. N. *Chem. Res. Toxicol*. **1998**, *11*, 710.

(15) Merenyi, G.; Lind, J.; Goldstein, S.; Czapski, G. *Chem. Res. Toxicol*. **1998**, *11*, 712.

(16) Lymar, S. V.; Hurst, J. K. *Chem. Res. Toxicol*. **1998**, *11*, 714.

(17) Koppenol, W. H. *Chem. Res. Toxicol*. **1998**, *11*, 716.

(18) Squadrito, G. L.; Pryor, W. A. *Chem. Res. Toxicol*. **1998**, *11*, 718.

(19) Radi, R. *Chem. Res. Toxicol*. **1998**, *11*, 720.

(20) Mahoney, L. R. *J. Am. Chem. Soc*. **1970**, *92*, 4244.

(21) Pryor, W. A.; Squadrito, G. L. *Am. J. Physiol.* **1995**, *288*, L699.

(22) Merenyi, G.; Lind, J. *Chem. Res. Toxicol*. **1997**, *10*, 1216.

(23) Koppenol, W. H.; Kissner, R. *Chem. Res. Toxicol.* **1998**, *11*, 87.

(24) Richeson, C. E.; Mulder, P.; Bowry, V. W.; Ingold, K. U. *J. Am. Chem. Soc*. **1998**, *120*, 7211.

(25) Hodges, G. R.; Ingold, K. U. *J. Am. Chem. Soc*. **1999**, *121*, 10695.

(26) Khan, A. U.; Kouccic, D.; Kulbanovek, A.; Desai, M.; Frenkel, K.; Geacintov, N. E. *Proc. Natl. Acad. Sci. U.S.A.* **2000**, *97*, 2984.

(27) Bartberger, M. D.; Fukuto, J. M.; Houk, K. N. *Proc. Natl. Acad. Sci. U.S.A.* **2001**, *98*, 2194.

(28) Merenyi, G.; Lind, J.; Czapski, G.; Goldstein, S. *Proc. Natl. Acad. Sci. U.S.A.* **2000**, *97*, 8216.

(29) Martinez, G. R.; Di Mascio, P.; Bonini, M. G.; Augusto, O.; Briviba, K.; Sies, H.; Maurer, P.; Rothlisberger, U.; Herold, S.; Koppenol, W. H. *Proc. Natl. Acad. Sci. U.S.A.* **2000**, *97*, 10307.

(30) Dixon, D. A.; Feller, D.; Peterson, K. A. *J. Phys. Chem.* **1997**, *101*, 9405; Feller, D.; Dixon, D. A.; Peterson, K. A. *J. Phys. Chem*. **1998**, *102*, 7053; Dixon, D. A.; Feller, D. *J. Phys. Chem. A* **1998**, *102*, 8209; Dixon, D. A.; Feller, D.; Sandrone, G. *J. Phys. Chem. A* **1999**, *103*, 4744; Feller, D.; Dixon, D. A. *J. Phys. Chem. A* **1999**, *103*, 6413; Feller, D.; Peterson, K. A. *J. Chem. Phys*. **1998**, *108*, 154; Feller, D.; Dixon, D. A. *J. Phys. Chem. A* **2000**, *104*, 3048; Feller, D. *J. Comput. Chem*. **1996**, *17*, 1571. The database is available at URL: http://www.emsl.pnl.gov: 2080/proj/crdb/.

(31) Purvis, G. D., III; Bartlett, R. J. *J. Chem. Phys*. **1982**, *76*, 1910; Raghavachari, K.; Trucks, G. W.; Pople, J. A.; Head-Gordon, M. *Chem. Phys. Lett*. **1989**, *157*, 479; Watts, J. D.; Gauss, J.; Bartlett, R. J. *J. Chem. Phys*. **1993**, *98*, 8718.

(32) Dunning, T. H., Jr. *J. Chem. Phys*. **1989**, *90*, 1007; Kendall, R. A.; Dunning, T. H., Jr.; Harrison, R. J. *J. Chem. Phys*. **1992**, *96*, 6796; Woon, D. E.; Dunning, T. H., Jr. *J. Chem. Phys*. **1995**, *103*, 4572.

(33) The calculations were done with MOLPRO-2000 (Werner, H. J.; Knowles, P. J.; Almlof, J.; Amos, R. D.; Berning, A.; Cooper, D. L.; Deegan, M. J. O.; Dobbyn, A. J.; Eckert, F.; Elbert, S. T.; Hampel, C.; Lindh, R.; Lloyd, A. W.; Meyer, W.; Nicklass, A.; Peterson, K. A.; Pitzer, R. M.; Stone, A. J.; Taylor, P. R.; Mura, M. E.; Pulay, P.; Schütz, M.; Stoll, H.; Thorsteinsson, T. MOLPRO-2000, Universität Stüttgart, Stüttgart, Germany, University of Sussex, Falmer, Brighton, England, 2000.), Gaussian 98 (Frisch, M. J.; Trucks, G. W.; Schlegel, H. B.; Scuseria, G. E.; Robb, M. A.; Cheeseman, J. R.; Zakrzewski, V. G.; Petersson, G. A.; Montgomery, J. A., Jr.; Stratmann, R. E.; Burant, J. C.; Dapprich, S.; Millam, J. M.; Daniels, A. D.; Kudin, K. N.; Strain, M. C.; Farkas, O.; Tomasi, J.; Barone, V.; Cossi, M.; Cammi, R.; Mennucci, B.; Pomelli, C.; Adamo, C.; Clifford, S.; Ochterski, J.; Petersson, G. A.; Ayala, P. Y.; Cui, Q.; Morokuma, K.; Malick, D. K.; Rabuck, A. D.; Raghavachari, K.; Foresman, J. B.; Cioslowski, J.; Ortiz, J. V.; Stefanov, B. B.; Liu, G.; Liashenko, A.; Piskorz, P.; Komaroni, I.; Gomperts, R.; Martin, R. L.; Fox, D. J.; Keith, T. A.; Al-Laham, M. A.; Peng, C. Y.; Nanayakkara, A.; Gonzalez, C.; Challacombe, M.; Gill, P. M. W.; Johnson, B. G.; Chen, W.; Wong, M. W.; Andreas, J. L.; Head-Gordon, M.; Replogle, E. S.; Pople, J. A. *Gaussian 98, A.7*; Gaussian, Inc.: Pittsburgh PA, 1998.), and *NWChem* (Anchell, J.; Apra, E.; Bernholdt, D.; Borowski, P.; Bylaska, E.; Clark, T.; Clerc, D.; Dachsel, H.; de Jong, B.; Deegan, M.; Dupuis, M.; Dyall, K.; Elwood, D.; Fann, G.; Fruchtl, H.; Glendening, E. D.; Gutowski, M.; Harrison, R.; Hess, A.; Jaffe, J.; Johnson, B.; Ju, J.; Kendall, R.; Kobayashi, R.; Kutteh, R.;

Lin, Z.; Littlefield, R.; Long, X.; Meng, B.; Nichols, J.; Nieplocha, J.; Rendall, A.; Rosing, M.; Sandrone, G.; Stave, M.; Straatsma, T.; Taylor, H.; Thomas, G.; van Lenthe, J.; Windus, T.; Wolinski, K.; Wong, A.; Zhang, Z. NWChem Version 3.3, 1999). All of the work was performed on an SGI Origin 2000 SGI PowerChallenge or the 512 processor IBM SP computer in the Molecular Sciences Computing Facility.

(34) Hampel, C.; Peterson, K. A.; Werner, H. J. *Chem. Phys. Lett*. **1990**, *190*, 1; Deegan, M. J. O.; Knowles, P. J. *Chem. Phys. Lett*. **1994**, *227*, 321; Knowles, P. J.; Hampel, C.; Werner, H. J. *J. Chem. Phys*. **1988**, *99*, 5219.

(35) Rittby, M.; Bartlett, R. J. *J. Phys. Chem.* **1988**, *92*, 3033; R/UCCSD-(T) is requested in MOLPRO by the keyword "UCCSD(T)" when combined with an ROHF wave function.

(36) Peterson, K. A.; Woon, D. E.; Dunning, T. H., Jr. *J. Chem. Phys*. **1994**, *100*, 7410.

(37) Møller, C.; Plesset, M. S. *Phys. Rev.* **1934**, *46*, 618; Pople, J. A.; Binkley, J. S.; Seeger, R. *Int. J. Quantum Chem. Symp*. **1976**, *10*, 1.

(38) Huber, K. P.; Herzberg, G. *Molecular Spectra and Molecular Structure: Vol. 4. Constants of Diatomic Molecules*; Van Nostrand Reinhold Co., Inc.: New York, 1979.

(39) Jacox, M. E. *J. Phys. Chem. Ref. Data*, Monograph No. 3, 1994.

(40) Shimanouchi, T. *J. Phys. Chem. Ref. Data* **1977**, *6*, 993.

(41) Pople, J. A.; Head-Gordon, M.; Raghavachari, K. *J. Chem. Phys*. **1987**, *87*, 5968.

(42) Lo, W. J.; Lee, Y. P. *J. Chem. Phys*. **1994**, *101*, 5494.

(43) Moore, C. E. "Atomic Energy Levels" Vol. NBS Circular 467, U.S. National Bureau of Standards, Washington, DC, 1949.

(44) Davidson, E. R.; Ishikawa, Y.; Malli, G. L. *Chem. Phys. Lett*. **1981**, *84*, 226.

(45) Chase, M. W., Jr. *NIST-JANAF Tables*, 4th ed.; *J. Phys. Chem. Ref. Data* Mono. 9, Suppl. 1, 1998; NIST WebBook. http://webbook.nist-.gov/

(46) Shum, L. G. S.; Benson, S. W. *J. Phys. Chem*. **1983**, *87*, 3479.

(47) Bauschlicher, C. W., Jr.; Partridge, H. *Chem. Phys. Lett*. **1993**, *208*, 241.

(48) DeMore, W. B.; Sander, S. P.; Golden, D. M.; Hampson, R. F.; Kurylo, M. J.; Howard, C. J.; Ravishankara, A. R.; Kolb, C. E.; Molina, M. J. "Chemical Kinetics and Photochemical Data for Use in Stratospheric Modeling," Evaluation Number 12, Jet Propulsion Laboratory (JPL) Publication 97-4, JPL, California Institute of Technology, Pasadena CA, 1997.

(49) Curtiss, L. A.; Raghavachari, K.; Trucks, G. W.; Pople, J. A. *J. Chem. Phys*. **1991**, *94*, 7221.

(50) McGrath, M. P.; Rowland, F. S. *J. Phys. Chem*. **1994**, *98*, 1061.

(51) Tsai, H. H.; Hamilton, T. P.; Tsai, J. H. M.; van der Woerd, M.; Harrison, J. G.; Jablonsky, M. J.; Beckman, J. S.; Koppenol, W. H. *J. Phys. Chem*. **1996**, *100*, 15087.

(52) Fukui, K. *Acct. Chem. Res*. **1981**, *14*, 363.

(53) Gonzalez, C.; Schlegel, H. B. *J. Chem. Phys.* **1989**, *90*, 2154; *J. Phys. Chem*. **1990**, *94*, 5523.

(54) Merenyi, G.; Lind, J.; Goldstein, S.; Czapski, G. *J. Phys. Chem. A* **1999**, *103*, 5685.

(55) Gerasimov, O. U.; Lymax, S. V. *Inorg. Chem*. **1994**, *38*, 4317.

(56) Schmidt, M. W.; Baldridge, K. K.; Boatz, J. A.; Elbert, S. T.; Gordon, M. S.; Jensen, J. H.; Koseki, S.; Matsunaga, N.; Nguyen, K. A.; Su, S. J.; Windus, T. L.; Dupuis, M.; Montgomery, J. A. *J. Comput. Chem.* **1993**, *14*, 1347.

(57) (a) Zhan, C.-G.; Bentley, J.; Chipman, D. M. *J. Chem. Phys*. **1998,** *108*, 177. (b) Zhan, C.-G.; Chipman, D. M. *J. Chem. Phys*. **1998**, *109*, 10543. (c) Zhan, C.-G.; Chipman, D. M. *J. Chem. Phys*. **1999**, *110*, 1611. (d) For the SVPE calculations at the MP2 level, the MP2 perturbation procedure was performed for the electron correlation correction after the converged HF wave function of solute in reaction field is obtained. (e) Once the solute cavity is defined and the dielectric constant is known, the accuracy of the SVPE numerical computation depends only on the number of surface nodes (N) representing the cavity surface and number of layers (M) describing the volume polarization charge distribution within a certain, sufficiently large three-dimensional space outside the solute cavity. If one could use an infinite number of nodes and an infinite number of layers, then the numerical results obtained from the SVPE computation would be exactly the same as those determined by the exact solution of the Poisson's equation for describing the solvent polarization potential. We have shown that the accuracy of the SVPE numerical computations employed in this study with $N = 590$ and $M = 10$ (for a step of 0.5 Å) is higher than that required for the results given in this paper.

(58) Zhan, C.-G.; Norberto de Souza, O.; Rittenhouse, R.; Ornstein, R. L. *J. Am. Chem. Soc*. **1999**, *121*, 7279.

(59) Zhan, C.-G.; Landry, D. W.; Ornstein, R. L. *J. Am. Chem. Soc*. **2000**, *122*, 2621.

(60) Zhan, C.-G.; Landry, D. W.; Ornstein, R. L. *J. Phys. Chem. A* **2000**, *104*, 7672.

(61) Parr, R. G.; Yang, W. *Density-Functional Theory of Atoms and Molecules*; Oxford University Press: New York, 1989.

(62) Stanbury, D. M. *Adv. Inorg. Chem*. **1989**, *33*, 69.

(63) Doclo, K.; Rothlisberger, U. *J. Phys. Chem A* **2000**, *104*, 6464.

(64) Bohle, D. S.; Hansert, B. *Nitric-Oxide-Bio. Chem*. **1997**, *1*, 502.

(65) Cameron, D. R.; Borrajo, A. M. P.; Bennett, B. M.; Thatcher, G. R. J. *Can. J. Chem*. **1995**, *73*, 1627.

(66) Sumathi, R.; Peyerimhoff, S. D. *J. Chem. Phys*. **1997**, *107*, 1872.

(67) Houk, K. N.; Condroski, K. R.; Pryor, W. A. *J. Am. Chem. Soc*. **1996**, *118*, 13002.

(68) Donahue, N. M.; Mohrschladt, R.; Dransfield, T. J.; Anderson, J. G.; Dubey, M. K. *J. Phys. Chem. A* **2001**, *105*, 1515.